Supporting Information

Simultaneous determination of acetaminophen and dopamine based on water-soluble pillar[6]arene and ultrafine Pd nanoparticles modified covalent organic framework nanocomposite

Xiaoping Tan, *[a] Tong Mu,[a] Sheng Wang,[a] Jian Li,[a] Juan Huang,[a] Huisheng Huang, *[a] Yan Pu,[a] Genfu Zhao *[b]

[a] Chongqing Key Laboratory of Inorganic Special Functional Materials, College of Chemistry and Chemical Engineering, Yangtze Normal University, Fuling 408100, China

[b] School of Materials and Energy, Yunnan Key Laboratory for Micro/Nano Materials and Technology, Yunnan University, No. 2, Green Lake North Road, Kunming 650091, China

S1 Instruments. The synthetic samples were characterized by Fourier transform infrared (FTIR) spectroscopy via the SCIENTIFIC Nicolet IS10 (Massachusetts, USA) and thermogravimetric analysis (TGA) (TA Instruments, New Castle, USA). EDS was carried out in the JEM 2100 transmission electron microscopy (TEM, Japan) equipped with an energy dispersive X-ray spectrometry. The crystallinity of prepared samples of COFs were characterized by powder X-ray diffraction (PXRD) and recorded using using a Bruker D8 Advance X-ray diffractometer at 40 kV and 40 mA over 2° to 80° 2θ range with a Cu Kα radiation. Gas adsorption measurement N_2 adsorption measurements were performed on a BELSORP II mini. Propane adsorption measurements were performed using a BELSORP-Max (BEL-Japan, Inc.). The X-ray photoelectron spectroscopy (XPS) was performed on an ESCALAB-MKII spectrometer (VG Co., United Kingdom) and with Al Ka X-ray radiation as the X-ray source for excitation. TEM images and the high resolution images were measured by a high resolution transmission electron microscope (HRTEM, JEM-2010). ^{1}H NMR and ^{13}C NMR spectra were recorded on a Bruker Avance DMX-400 spectrometer at 500 MHz. Electrochemical measurements were obtained from a CHI660E electrochemical workstation (Shanghai Chenhua Instrument Co. Ltd., China) with conventional three-electrode system, including a modified glassy carbon working electrode (GCE), a saturated calomel reference electrode (SCE) and a Pt wire auxiliary electrode.

S2 Electrochemical simultaneous determination of AP and DA. Firstly, the clean bare electrodes (GCEs) were prepared by polishing and cleaning with alumina powder and ultrapure water, respectively. Modified GCE of WP6-COF-Pd/GCE was prepared by dropping the dispersed solution of WP6-COF-Pd in ethanol (6.0 μL) onto the surface of the apinoid GCE and dried naturally. Other modified GCE of Pd-COF/GCE was prepared with similar procedure of WP6@Ag@COF/GCE, in which WP6-Pd-COF was replaced by COF and Pd-COF. The determination of AP and DA via WP6-Pd-COF/GCE was carried out by differential pulse voltammetery (DPV) technique with working potential from -0.2 to 0.8 V in PBS (0.1 M pH 7.0) containing different concentrations of AP and DA. For studying the reproducibility and stability of the

developed electrochemical sensing system of WP6-Pd-COF/GCE, all electrochemical measurements were implemented at least five times. All electrochemical measuring is carried out by CHI660E electrochemical workstation.

S3 Synthesis of water-soluble pillar[6]arene (WP6)[1-3]

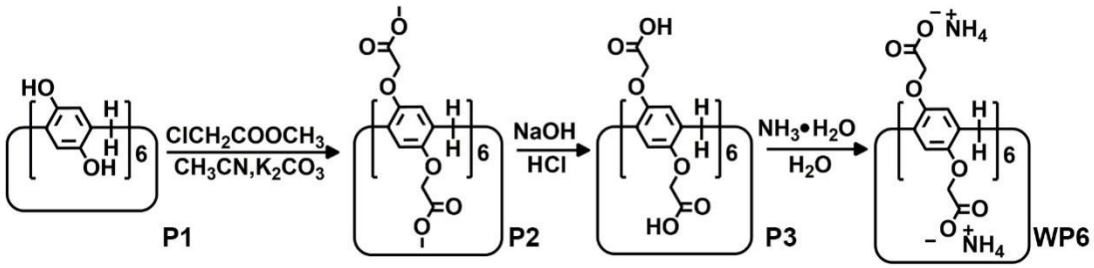

Scheme S1. Synthetic route of **WP6**.

S4 Synthesis of compound A[4]

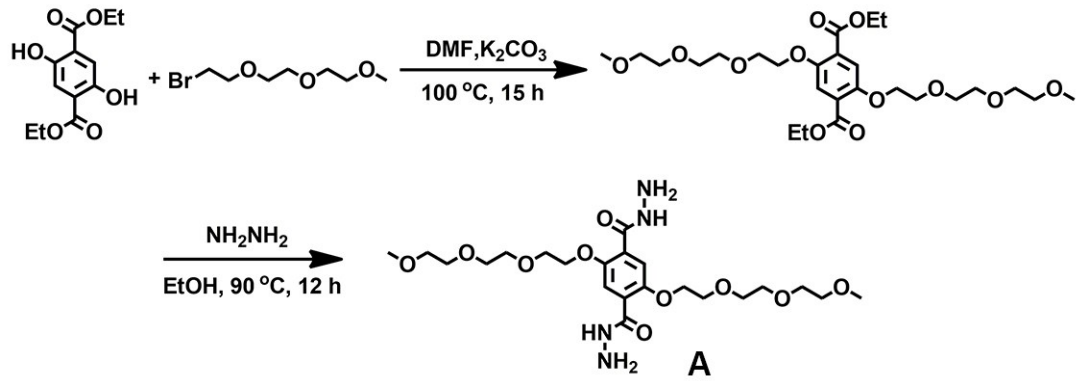

Scheme S2. Synthetic route of **A**.

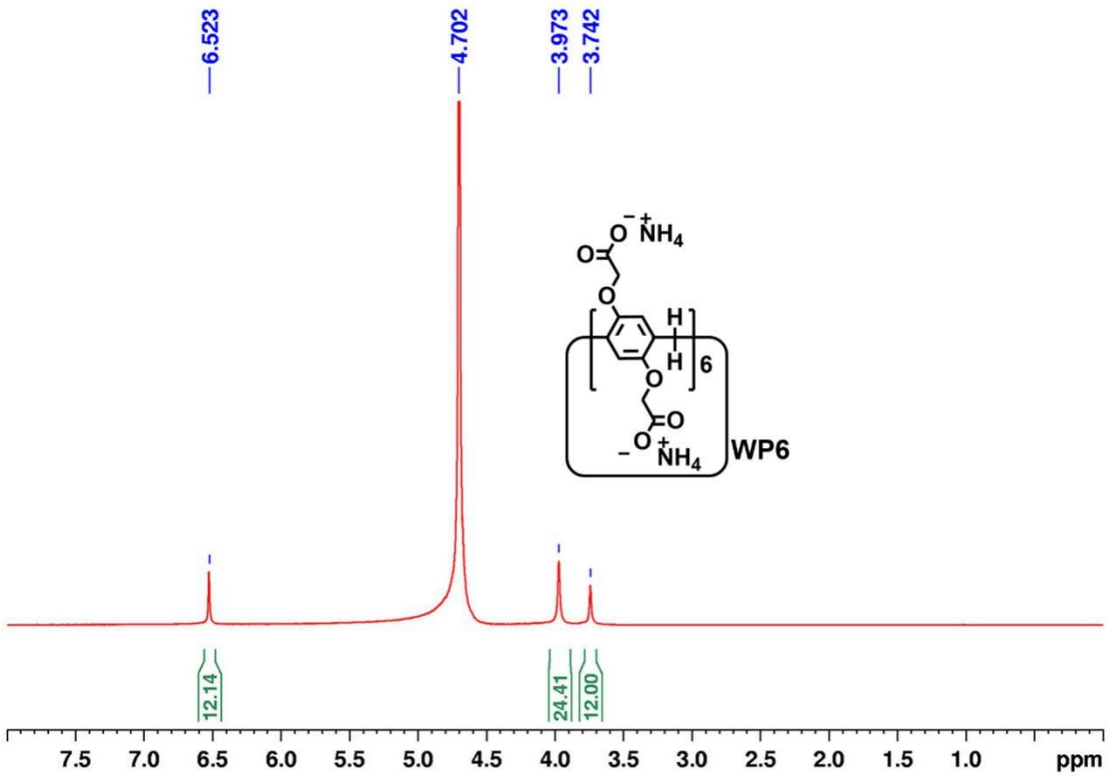

Figure S1. ^{1}H NMR spectrum (500 MHz, D_2O, 298 K) of **WP6**.

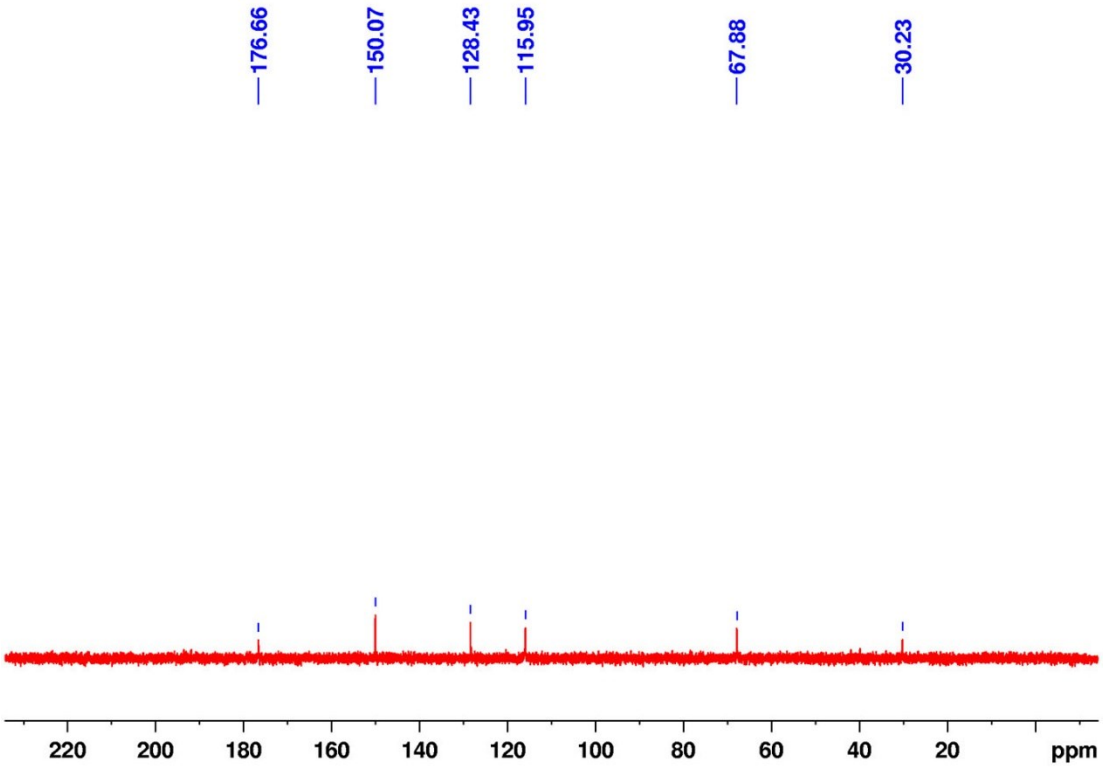

Figure S2. ^{13}C NMR spectrum (125 MHz, D_2O, 298 K) of **WP6**.

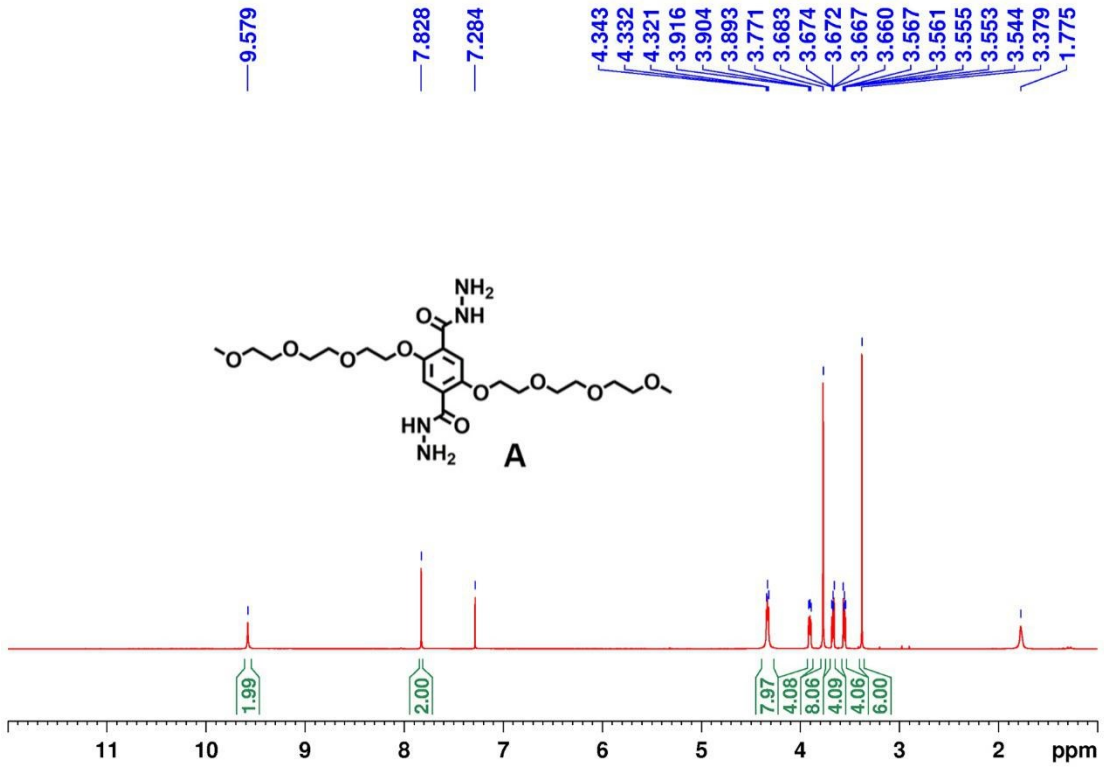

Figure S3. ^{1}H NMR spectrum (500 MHz, $CDCl_3$, 298 K) of **A**.

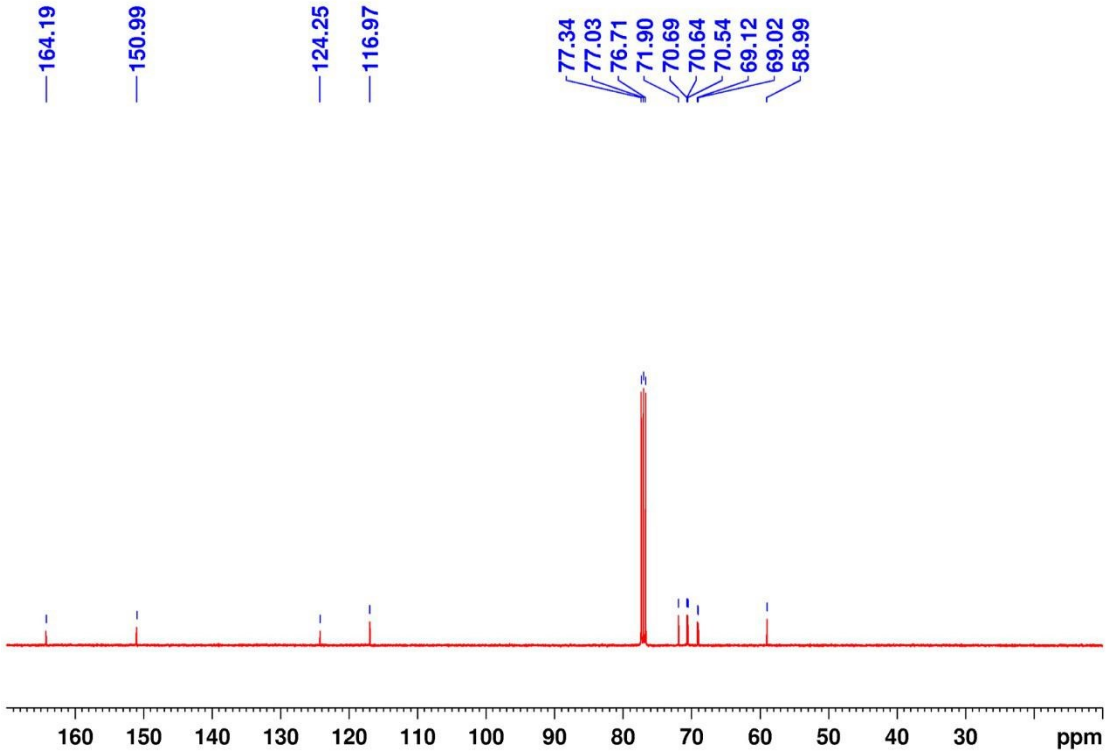

Figure S4. ^{13}C NMR spectrum (125 MHz, $CDCl_3$, 298 K) of **A**.

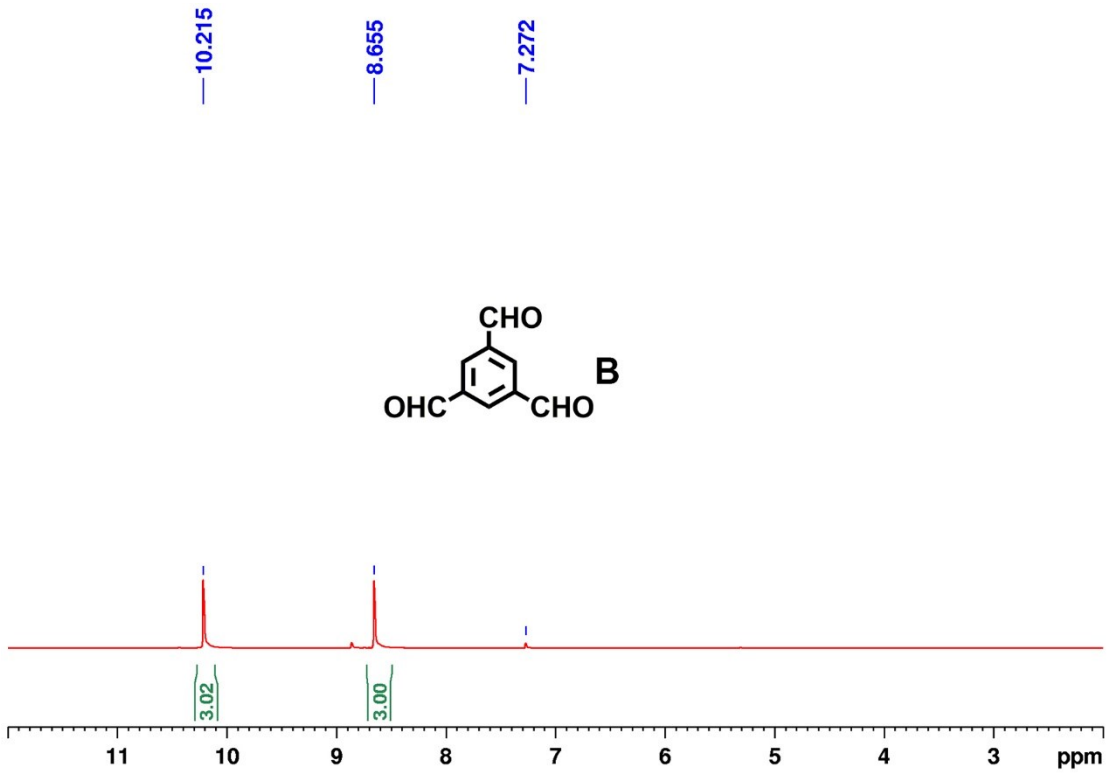

Figure S5. ^{1}H NMR spectrum (500 MHz, $CDCl_3$, 298 K) of **B**.

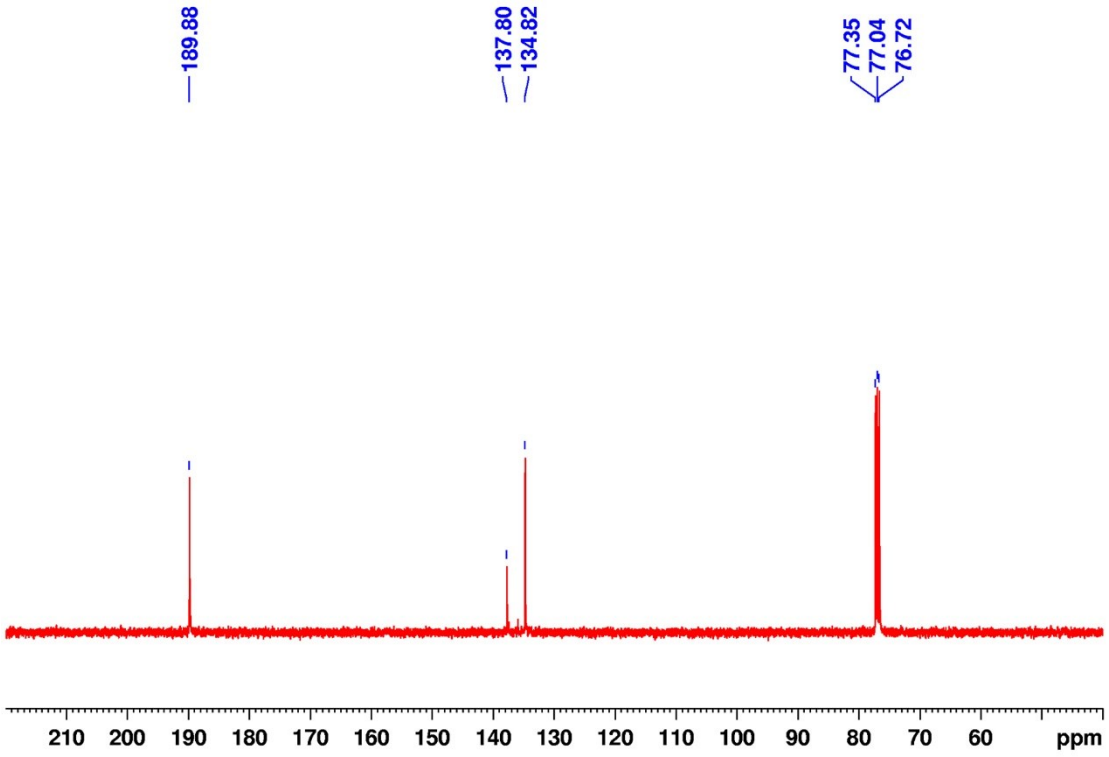

Figure S6. ^{13}C NMR spectrum (125 MHz, $CDCl_3$, 298 K) of **B**.

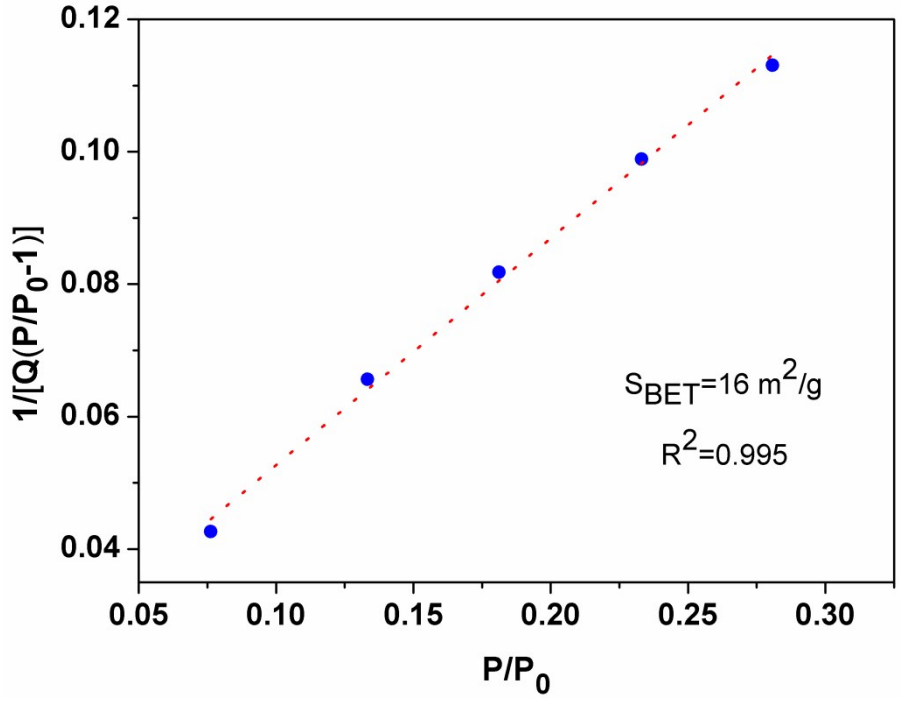

Figure S7. BET plot of COF

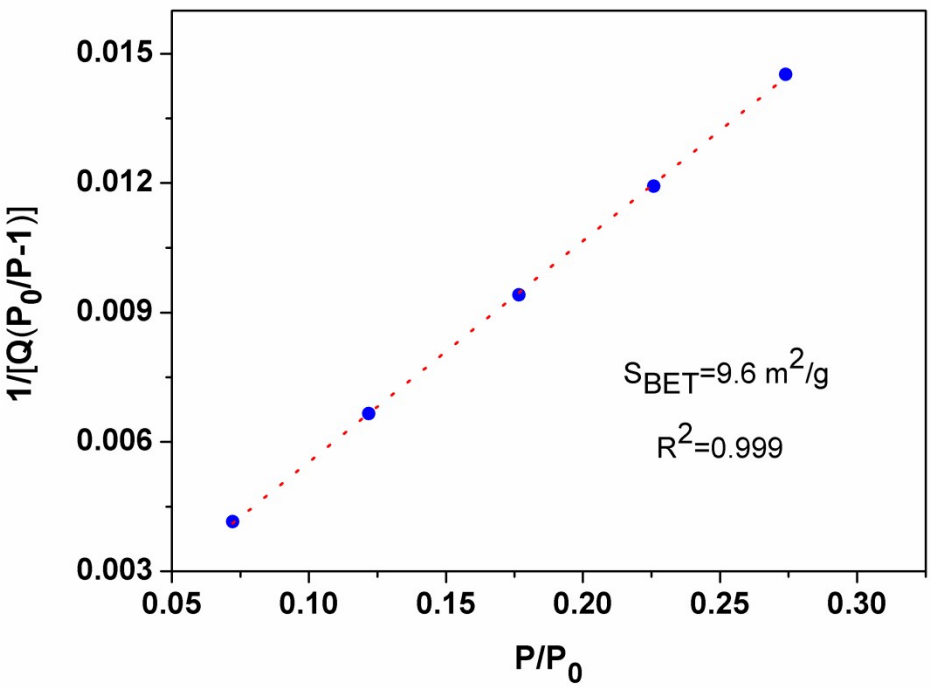

Figure S8. BET plot of WP6-COF-Pd.

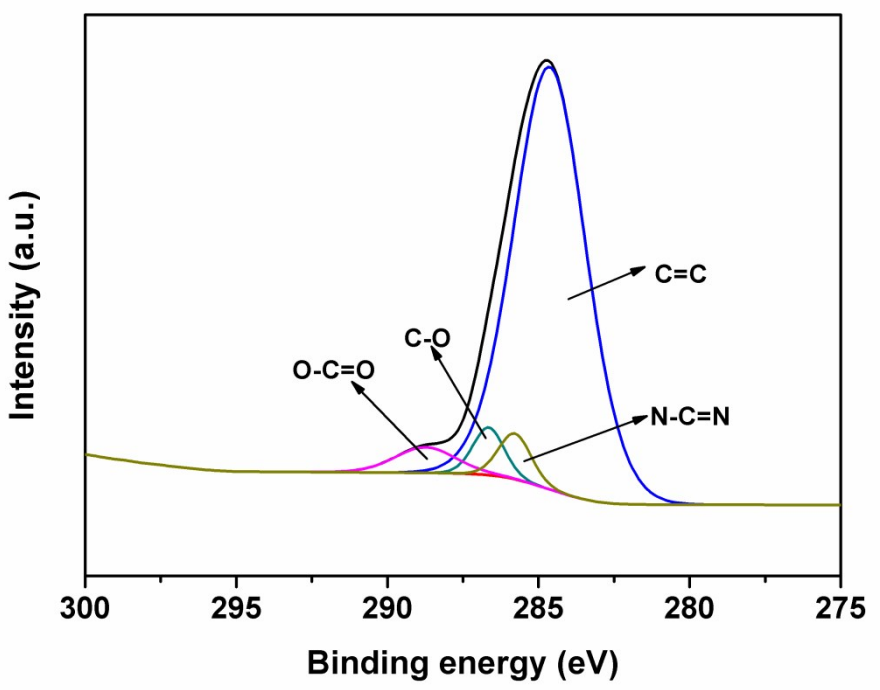

Figure S9. High resolution XPS spectrum of C 1s for WP6-Pd-COF.

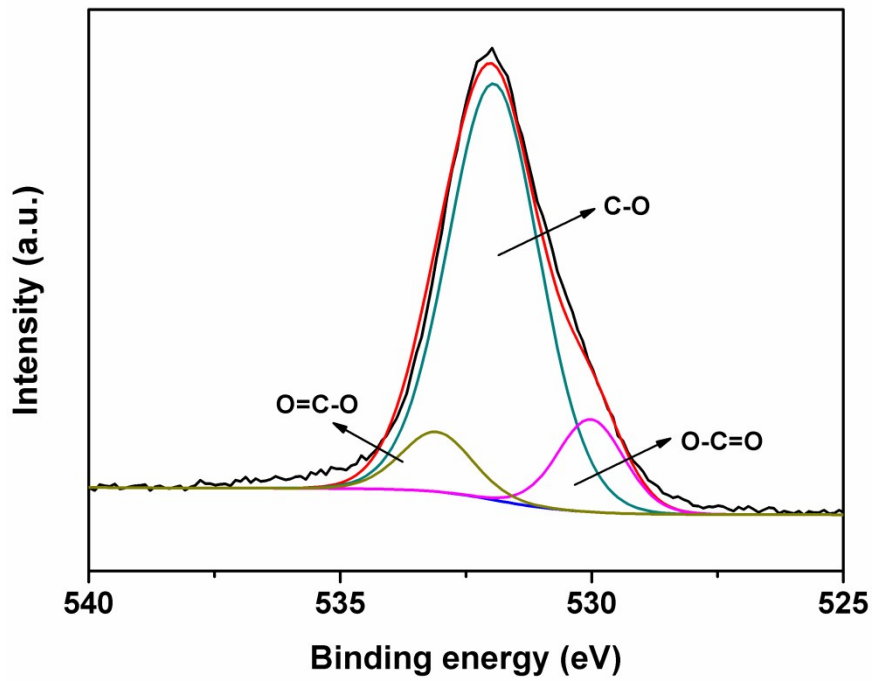

Figure S10. High resolution XPS spectra of C 1s for WP6-Pd-COF.

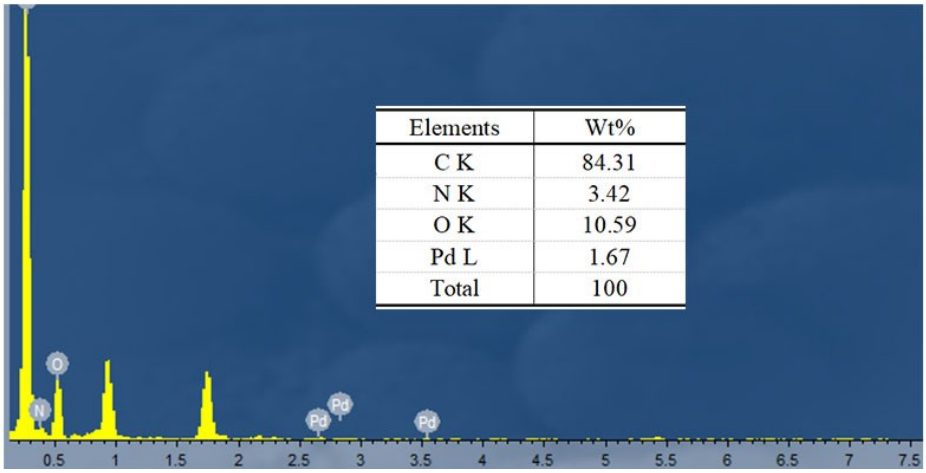

Figure S11. EDX spectrum of WP6-Pd-COF.

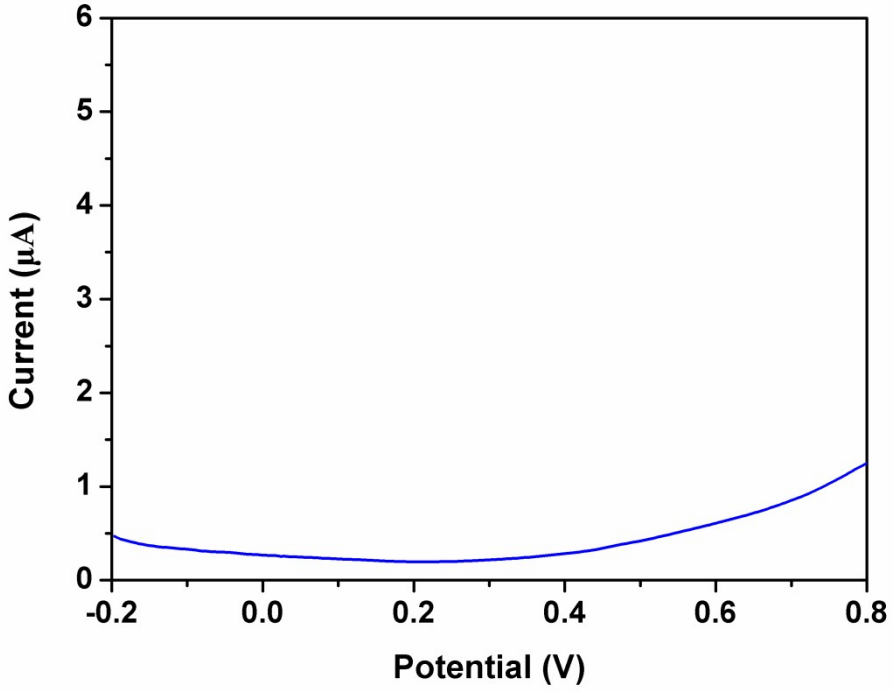

Figure S12. DPV response curve of WP6-Pd-COF modified electrode at the 0.1 M pH 7.0 PBS solution in the absence of DA and AP.

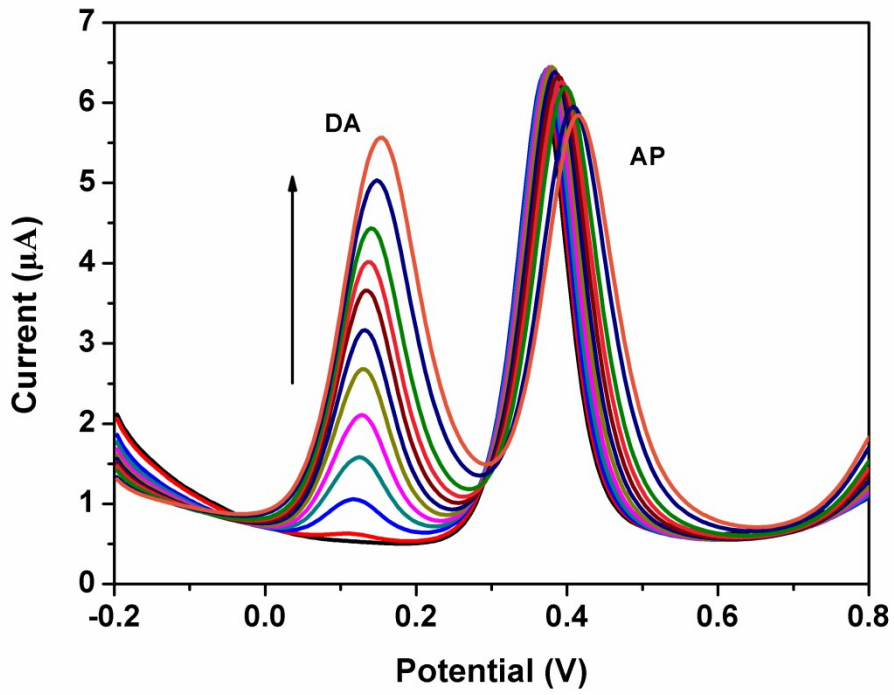

Figure S13. DPV curves obtained for DA (concentrations: 0.2, 0.6, 1.2, 1.8, 2.8, 3.6, 4.4, 5.0, 6.0, 7.0 and 8.0 μM) in the presence of 6.0 μM of AP at WP6-Pd-COF modified electrode in 0.1 M pH 7.0 PBS solution.

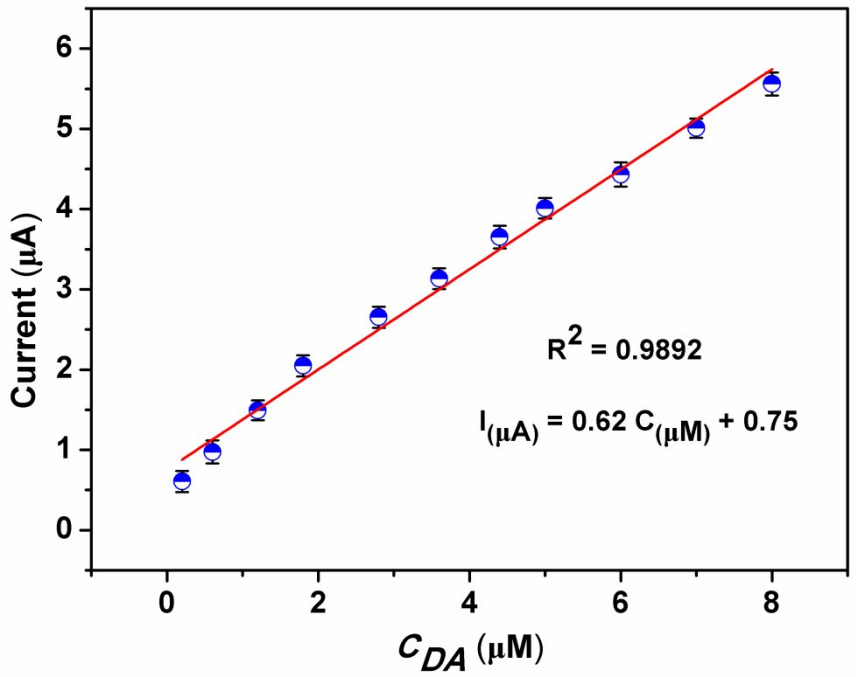

Figure S14. Calibration plots for determination of DA.

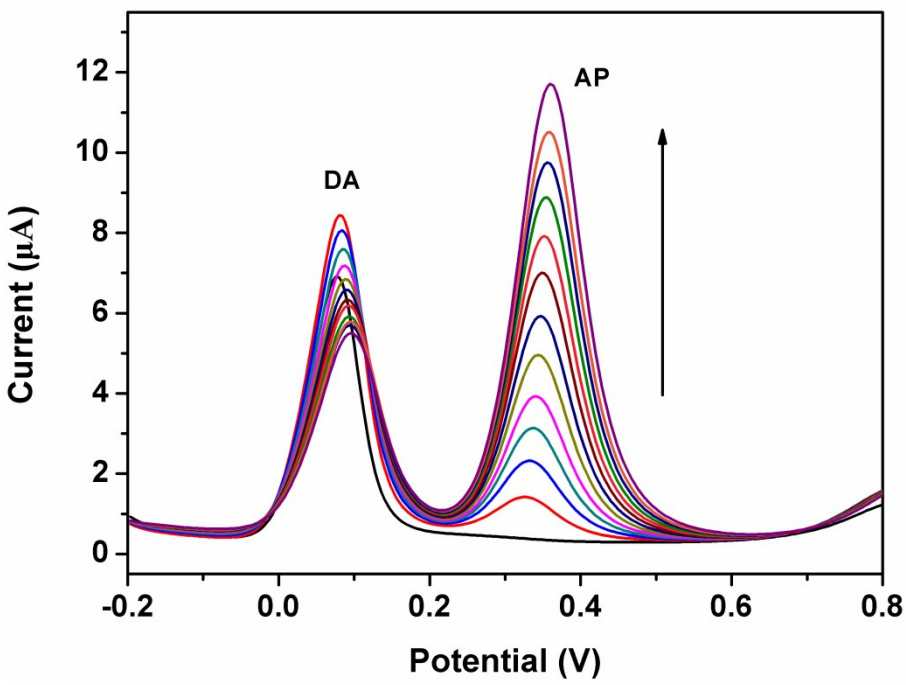

Figure S15. DPV curves obtained for AP (concentrations: 0.2, 0.5, 0.8, 1.2, 1.5, 2.0, 2.8, 3.6, 4.0, 4.5, 5.0 and 6.0 μM) in the presence of 6.0 μM of DA at WP6-Pd-COF modified electrode in 0.1 M pH 7.0 PBS solution.

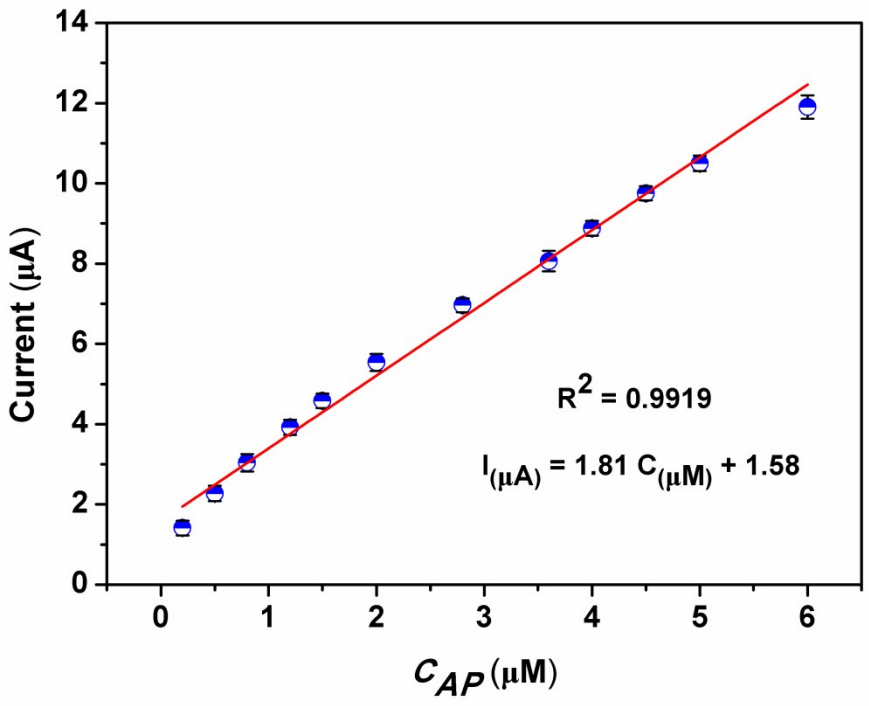

Figure S16. Calibration plots for the determination of AP.

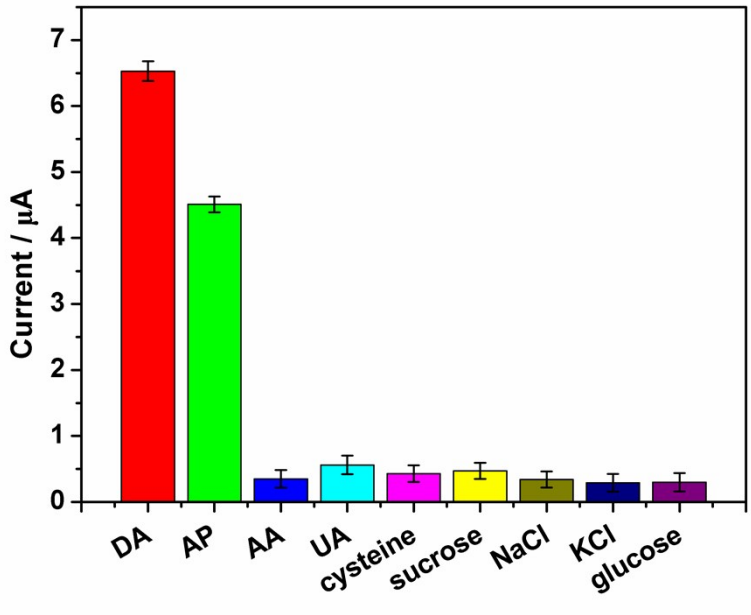

Figure S17. The selectivity for detection DA (4.0 μM) and AP (4.0 μM).

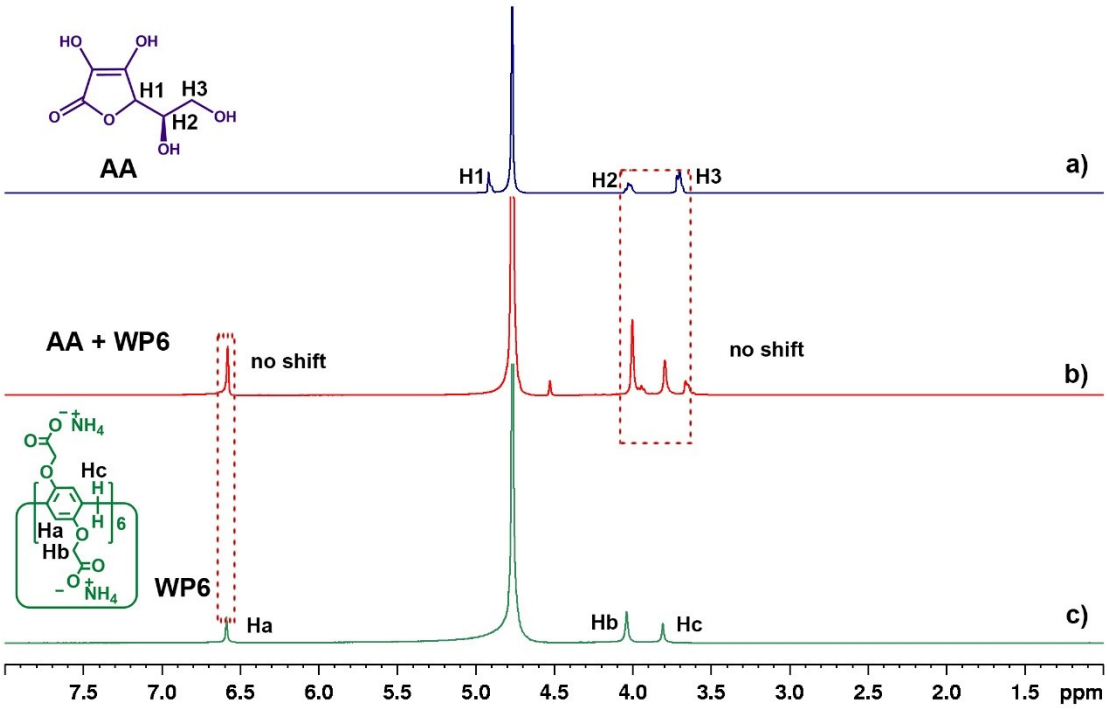

Figure S18. Host-guest ^{1}H NMR spectra of 10.0 mM AA (a), 10.0 mM AA + 10.0 mM WP6 (b) and 10.0 mM WP6 (c).

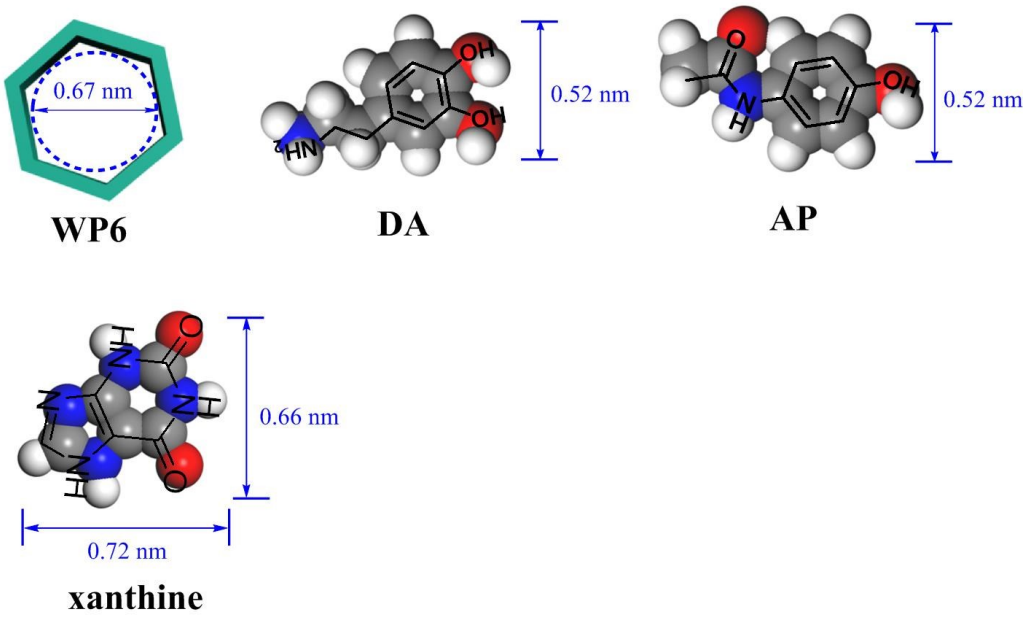

Figure S19. Cavity size of WP6 [5], and molecule size of DA, AP and xanthine (the size is measured by Materials Studio), respectively.

Table S1. Comparison of the proposed WP6-Pd-COF with reported electrochemical detection of DA and AP.

Modified electrode	Target analyte	Liner range (μM)	LOD (μM)	Ref
Pt/CeO_2@Cu_2O−CPE	DA	0.5-160	0.07	6
	AP	0.5-160	0.09	
MWCNT/GCE	DA	3-200	0.8	7
	AP	3-300	0.6	
pyrolytic carbon film	DA	18-270	2.3	8
	AP	15-225	1.4	
Ppyox/Az/Au	DA	0.1-30	0.05	9
	AP	0.2-100	0.08	
SWCNT	DA	3-200	0.05	10
	AP	0.5-100	0.08	
WP6-Pd-COF	DA	0.2-8	0.06	This work
	AP	0.1-7.5	0.03	

Table S2 Determination of DA and AP in urine sample (n = 3).

Sample	Added (μM)	Found (μM)	RSD (%)	Recovery (%)
DA	1.0	0.97 ± 0.02	2.06	97.0
	2.0	1.95 ± 0.13	6.6	97.5
	4.0	4.03 ± 0.15	3.7	100.7
AP	1	1.02 ± 0.03	2.9	102.0
	3	2.96 ± 0.15	5.06	98.6
	6	5.86 ± 0.23	3.92	97.6

References

1 T. Ogoshi, M. Hashizume, T. A. Yamagishi, Y. Nakamoto, *Chem. Commun*., 2010, **46**, 3708–3710.

2 G. C. Yu, M. Xue, Z. B. Zhang, J. Y. Li, C. Y. Han, F. H. Huang, *J. Am. Chem. Soc*., 2012, **134**, 13248−13251.

3 M. X. Wu, H. J. Yan, J. Gao, Y. Cheng, J. Yang, J. R. Wu, B. J. Gong, H.-Y. Zhang, Y. W. Yang, *ACS Appl. Mater. Interfaces*, 2018, **10**, 34655−34663.

4 G. Zhang, Y.-L. Hong, Y. Nishiyama, S. Bai, S. Kitagawa, S. Horike, *J. Am. Chem. Soc*., 2019, **141**, 1227−1234.

5 T. Ogoshi, S. Takashima, T. Yamagishi, *J. Am. Chem. Soc*., 2015, **137**, 10962–10964.

6 A. R. Rajamani, S. C. Peter, *ACS Appl. Nano Mater*., 2018, **1**, 5148−5157.

7 Z. A. Alothman, N. Bukhari, S. M. Wabaidur, S. Haider, *Sens. Actuators, B*, 2010, **146**, 314−320.

8 G. P. Keeley, N. McEvoy, H. Nolan, S. Kumar, E. Rezvani, M. Holzinger, S. Cosnier, G. S. Duesberg, *Anal. Methods*, 2012, **4**, 2048−2053.

9 M. B. Gholivand, M. Amiri, *J. Electroanal. Chem*., 2012, **676**, 53−59.

10 B. Habibi, M. Jahanbakhshi, M. H. P. Azar, *Electrochim. Acta*, 2011, **56**, 2888–2894.